Optimization of the Paint Shop Curing Process Using Simcenter STAR-CCM+

Tiago Augusto Santiago Vieira
Davi Machado Cury
Pedro Henrique Araujo
Aline Amaral Quintella Abdu
Caiuã Caldeira de Melo
Fábio de Castro Orefice
Henrique Carlos Monteiro
Siemens Digital Industries Software

ABSTRACT

The automotive industry increasingly relies on simulation tools for product development, enhancing safety, trustworthiness, and sustainability. Computational Fluid Dynamics (CFD) is widely used for vehicle aerodynamics and engine thermal management, but its application in manufacturing engineering continues to expand. Paint curing, a highly energy-intensive process in automotive manufacturing, benefits from CFD modeling to promote energy conservation, sustainability, and reduce greenhouse gas emissions. This study improved a previously developed paint oven model using Simcenter STAR-CCM+ to reduce heat loss and enhance product quality. The initial model used a surrogate Body-in-White (BIW) with a refined overset mesh in motion within the oven's background mesh, incorporating a shell thickness parameter to reduce computational complexity and cost. Intense heat transfer on the skid transport was observed due to re-circulation near the transition zone between hot and cold oven sections. The transition zone was redesigned to improve heat transfer to the BIW instead of the skid, resulting in less energy loss to the skid. Additionally, more BIWs were added to the simulation to understand their mutual influence.

INTRODUCTION

In the automotive industry, enhancing process efficiency to maximize outcomes is an increasingly challenging task, essential for companies to thrive in the current globalized competitive market. Production, quality, costs, environmental impact, social responsibility, and safety are critical vectors inherent in any process. Maximizing results necessitates the optimal alignment of these variables to achieve synergy. Furthermore, energy consumption is a significant concern for companies due to its direct correlation with costs and environmental issues, such as greenhouse gas emissions [1].

Energy efficiency represents the most effective strategy to combat climate change. Within the context of automotive manufacturing, enhancing energy efficiency is of paramount importance. Despite the modern and relatively efficient nature of many contemporary automotive manufacturing facilities, significant opportunities exist for substantial energy savings and favorable environmental impacts [2].

The Body in White (BIW), which constitutes the vehicle's structure, undergoes painting in an automotive assembly paint shop. This painting process involves multiple operations and layers of various coatings for both protection and aesthetics, necessitating repeated painting and drying operations [3].

Ovens are employed to bake and cure the paint layers on the BIW. These ovens, extending hundreds of meters in length, utilize radiation and/or convection to heat the BIW. Accurately predicting the temperature over time at different BIW locations as it traverses the oven is crucial for assessing the paint quality. Typically, these ovens are divided into multiple zones to heat, maintain, and subsequently cool the bodies. These zones may feature heated walls or nozzles that blow hot air onto the BIW [4].

During the curing process, the paint solvent vaporizes, the solids form molecular bonds, and the paint layers cure. The quality of the paint and adhesives on a finished vehicle is largely dependent on this curing process. It is critical to fully cure the paint and adhesives on all BIW parts. However, due to the complex geometry of the BIW, the heat received, and the temperature rise over time vary significantly between different parts and regions [5].

Among the various stages of automobile manufacturing, the painting process is the most energy-intensive, primarily due to the energy required for heating the booths and ovens. Consequently, selecting the appropriate oven and its features can lead to significant reductions in energy consumption and costs [2].

Figure 1 illustrates the total energy consumption of a conventional automotive manufacturing plant, segmented into the paint shop, press shop chassis, powertrain, transmission and engine assembly, body shop, and final assembly. The painting and oven sections account for the highest energy consumption during vehicle manufacturing processes. The paint shop is crucial as it provides the BIW with an aesthetically pleasing finish and protection against weather and corrosion, underscoring its importance [6].

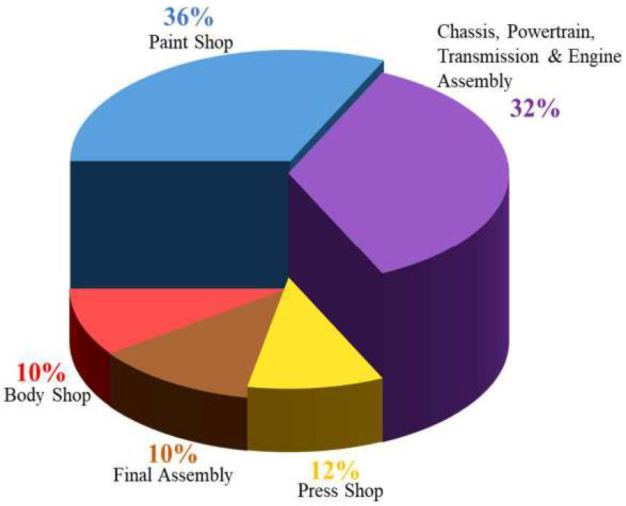

Figure 1 – Relative energy consumption per manufacturing process in automotive industry [6].

Failures in the painting process require rework, which increases production costs and may necessitate delivering a new vehicle to the customer in the event of a recall. To ensure painting quality, engineers often adjust the temperature of each chamber in the painting unit based on empirical observations, as the quality of the painting is significantly affected by the uniform distribution of temperature within the oven and the conveyor speed, which is directly related to production. Thus, the relationship between production, energy consumption, and quality is crucial for making informed decisions [1].

In some cases, particularly due to increased production rates or the introduction of new car models, existing ovens in car factories may struggle to maintain adequate indoor air temperatures. Before releasing a new vehicle model, almost every car manufacturer faces concerns about whether the paint can be properly cured within the existing or new paint cure ovens, and how the existing oven can be modified to meet the paint cure requirements. To address these concerns, manufacturers must either purchase new ovens or retrofit and redesign existing facilities. In either case, simulating oven operations under various conditions is essential, as oven temperature directly affects the final paint quality [2].

Typically, adjustments to chamber temperatures are made conservatively, resulting in higher energy consumption. Therefore, it is crucial to examine and develop a representative model of the drying/curing process to understand and optimize it, thereby preventing failures and reducing energy costs [1].

Physical tests to determine the curing level on vehicle components are often non-predictive, costly, and time-consuming. Therefore, it is essential to use temperature-time history predictions of a BIW to evaluate the paint quality and ascertain the manufacturability of a vehicle design within an existing paint oven [7].

The complex geometry of the oven and its components, along with the numerous parameters that affect the curing process, complicate the design of such ovens. The design of these ovens, used for complex geometries such as auto bodies, generally relies on trial and error. This method is typically time-consuming and impractical for problems with many influencing parameters. Nowadays, due to advancements in computational power, researchers are increasingly focusing on simulation methods to prevent that, and several studies have been conducted in this area [6].

To address the limitations of physical tests, simulations have become a valuable alternative. Through process and product modeling, behavior can be predicted, and potential issues can be anticipated and avoided. In the automotive industry, simulations are increasingly used to reduce production waste and enhance the final product. Computational Fluid Dynamics (CFD) is a widely employed method for paint shop analysis, including dipping, e-coat, and draining, as well as subsequent paint shop processes such as paint curing [8].

During the curing process, the BIW undergoes a heating phase, which must maintain the BIW parts at a temperature threshold long enough for the paint to achieve its desired properties. Subsequently, the BIW enters a cooling phase, reducing the temperature for the next process. Both phases can be modeled using CFD calculations, providing insights into the BIW temperature evolution during the process and the adequacy and impact of the process on the product [9].

In previous work [10], a paint oven model was developed and evaluated using Simcenter STAR-CCM+ [11]. The model was constructed using a generic BIW with a refined overset mesh moving within a coarse oven background mesh. The metal sheet thickness was considered using a shell thickness parameter, a meshless approach that reduces computational complexity and cost. The initial model was analyzed, outlining the components' temperature variation and facilitating an understanding of the curing process and the applied paint quality.

This study enhanced a previously developed paint oven model using Simcenter STAR-CCM+ to reduce heat loss and improve product quality. The initial model, which used a dummy BIW with a refined overset mesh, revealed intense heat transfer to the skid due to re-circulation near the transition zone. By redesigning the transition zone to alter the flow direction from bottom to top, heat transfer to the BIW was improved, reducing energy loss to the skid. Additionally, incorporating more BIWs into the simulation helped to understand their mutual influence, leading to a more comprehensive and realistic representation of the oven's performance under typical operational conditions.

METHODOLOGY

The methodology for curing simulation involves three primary stages: preparing the geometry and meshing (for both oven and BIW), setting up the simulation (which includes constructing an overset mesh, defining motion, and establishing boundary conditions), and post-processing.

The oven geometry was modeled based on an actual automotive oven, with adjustments to its dimensions and boundary conditions. BIW geometry was simplified to effectively demonstrate the concept of the developed methodology.

In a previous study, the oven's length was greater, with the same dimensions for the hot and cold sections. However, it was found that the cold section could be reduced without affecting performance. Additionally, the transition zone was configured with a hot flow from top to bottom through specific inlets and outlets placed vertically inside the oven. This setup created a large vortex at the top of the hot side near the transition zone, resulting in a higher velocity of airflow counter to the BIW movement. This behavior was expected to enhance heat transfer at the bottom of the BIW assembly and skid, leading to heat loss to the skid.

To address these potential improvements, the cold section of the oven was reduced, and the flow direction in the transition zone was reversed. The transition zone flow now occurs from bottom to top instead of top to bottom. This change is expected to reduce the size of the vortex and position it at the bottom interface between the hot side and the transition zone, thereby increasing heat transfer to the BIW areas of interest rather than the skid.

GEOMETRY AND MESH - As our previous work [10], the utilized BIW geometry was simplified in terms of number of metal sheets and structural materials in comparison to an actual BIW. However, it contains all main parts and characteristics that impact the curing process. Besides, the transport skid was also employed to the model, since it is a important part that drains part of the energy inserted into the oven. The BIW and its corresponding Skid are depicted in Figure 2. In addition to the previously developed work [10], two more BIWs were added to the domain, one ahead and the other behind the monitored BIW. This should significantly change the flow behavior around the monitored BIW, leading to a more realistic condition, which allows the understanding of the impact these additional products have on the temperature evolution of the monitored BIW.

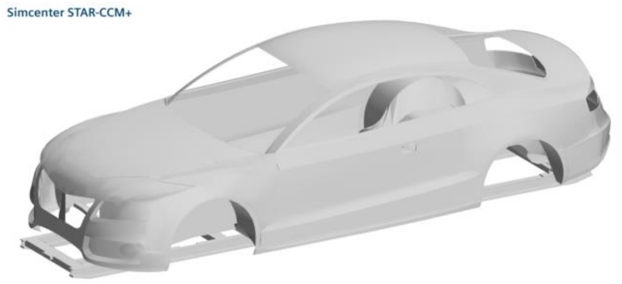

Figure 2. BIW and transport Skid geometries [10].

The curing oven geometry, as illustrated in Figure 3, outlines the three zones through which the BIW passes. The first zone is the heating zone, where hot air is injected through each nozzle at a speed of 10 m/s and a temperature of 500 K. The objective of the heating zone is to equalize the BIW temperature according to the paint cure properties, which vary by manufacturer [12]. Outlet ducts are periodically placed on the top wall of the heating zone to facilitate air exchange and renewal.

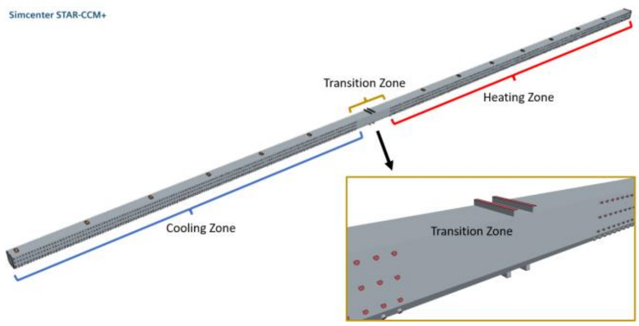

Figure 3. Cure oven geometry.

Next is the transition zone, which is designed to minimize heat loss from the heating zone to the cooling zone. The transition zone serves to isolate the heating and cooling zones from each other. Within the transition zone, there are two hot air blowers on the top wall of the oven and two outlet ducts on the bottom wall. The hot air blowers are expected to create a barrier that prevents air from the heating zone from mixing with air in the cooling zone. Without the transition zone, this mixing effect would inevitably occur due to the different temperature potentials. The transition blowers supply the oven with air at a flow rate of 50 m/s and a temperature of 500 K. As attested earlier, the flow direction in the transition zone was altered, so that it now moves from bottom to top instead of top to bottom. This adjustment is expected to decrease the vortex size and position it at the lower interface between the hot side and the transition zone, thereby enhancing heat transfer to the BIW areas of interest rather than the skid.

The last section of the curing oven is the cooling zone, which is designed to bring the BIW back to ambient temperature. The cold air blowers in this zone are built to the same specifications as those in the heating zone. To facilitate air exchange and renewal, outlet ducts are periodically placed along the top wall of the cooling zone.

The oven geometry of the current work was changed to achieve better results. First, the length of the oven was shortened in the cooling zone. This was assumed given that in the previous work [10], the BIW was cooled before passing through the entire length of the cooling zone. Then the vertical length of the oven decreased, since the roof was hotter than the rest of the BIW in the previous work. Finally, the horizontal length of the oven was enlarged to allow better flow distribution, avoiding heat transfer to the transport skid. Figure 4 shows a section of the combined mesh of the BIW and the oven for the current work and the previous one.

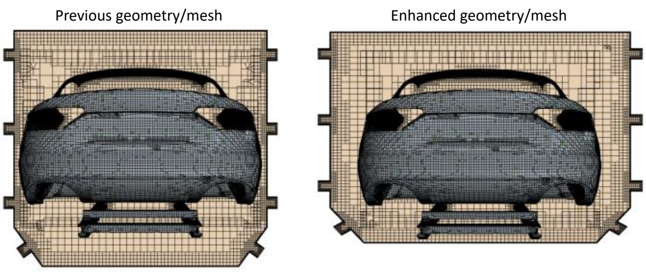

Figure 4. Previous and current (enhanced) geometries/meshes.

Following the process of geometry preparation, both domains (the BIWs and the curing oven) underwent discretization, resulting in the generation of two distinct meshes. The curing oven mesh consists of approximately 35 million cells, while the mesh of each added BIW comprises 2,379,562 cells. The oven mesh is smaller than the previous work due to the smaller length of the cooling zone. The oven mesh was regenerated to achieve more homogeneous cell sizes, which improves the numerical stability, since BIWs meshes movement will cause less changes in comparison to previous works.

The overset mesh of the BIWs was modified to include a shell region representing the metal sheets. This shell region required specifying the thickness of the metal sheets, which were set at 1.0 mm instead of the previous value of 3.5 mm. The current value reflects better the sheets thickness used in the automotive industry. Although it is possible to vary this parameter according to the specific BIW part, the thickness was kept uniform for all BIW parts in this proof-of-concept study. The shell region consists of a mesh with a thickness of one cell [11], resulting in a mesh with 328,817 cells in this case. The BIW mesh was then integrated within the baking oven mesh, creating an overlapping, or overset, mesh. This process and the resulting mesh are depicted in Figure 5.

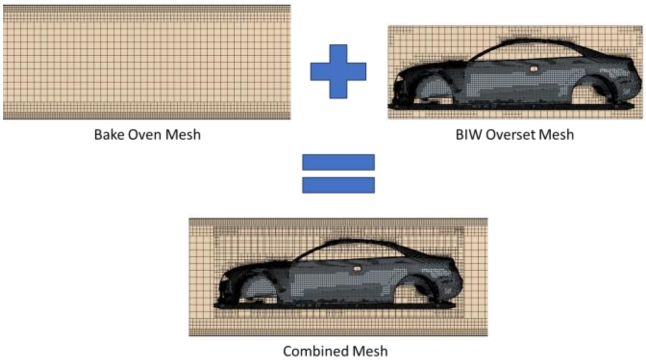

Figure 5. Meshes union process, forming the combined mesh [10].

Figure 6 shows the combined mesh used in the current work with two additional BIWs inside the oven mesh. As can be seen, the differences between the BIWs meshes and the oven one is lower than the previous work (see Figure 5). The distance between each BIW was 2 meters.

Figure 6. Combined mesh with three BIWs.

BOUNDARY CONDITIONS - The simulation conducted is inherently transient due to the nature of the process being modeled, requiring time discretization and evolution throughout the simulated process. To maintain a stable Courant Flow Number (CFN), a time step of 1 second was employed. Although this might be considered high from an academic perspective, concessions were made to ensure industrial feasibility, given that the curing oven process can last close to an hour. Consequently, coarse time and space discretization were selected. Despite this, the results provided detailed temperature data for the curing oven and the BIW during the paint curing process. While an adaptive time step can be utilized in Simcenter STAR-CCM+, it can be computationally expensive as the time step decreases to keep the CFN within the configured range, potentially impacting the total simulation time adversely in the event of minor numerical instability.

The movement of the BIW was defined using a CSV file, which included the linear velocity of the BIW in the oven length direction. The velocity used was 0.10 m/s, corresponding to a production line velocity of 6 BIWs per hour. The combination of mesh refinement level, BIW velocity, and time step ensures simulation stability. If the oven mesh is too fine compared to the BIW mesh, interpolation between the two meshes may cause the simulation to crash due to severe transients with high refinement differences. Additionally, the time step must align with the BIW velocity, as the overset mesh morphs the oven mesh during this process.

The time step size is dictated by the transient phenomena being modeled, capturing the flow's transient behavior at a desired frequency. When using overset meshes, an additional criterion for choosing the time step size is required. If an inactive cell becomes active without being an acceptor cell for at least one timestep, there is no solution from the previous time step at that cell to compute the rate of change term. Since the time integration was set to the first-order Euler scheme, the maximum movement is the smallest cell in the overlapping zone, as the scheme requires one previous time step value [11]. The total physical time simulated was 1650 seconds, requiring approximately 24 hours of computation using 240 cores.

The velocity of the nozzles in the heating and cooling zones was 10 m/s. The temperature of the nozzles in the heating zone was 500 K, while the temperature in the cooling zone was 300 K. The outlet ducts were set as pressure outlets with zero pressure. The oven walls were set as no-slip walls with convective losses to the environment, using a convective coefficient of 10 W/m²K and an outside temperature of 300 K. This is a conservative approximation, as such ovens typically have insulators to maintain internal temperature and conserve burner energy.

RESULTS

The achieved results are divided into two parts. The first part concerns the oven's behavior in terms of its temperature and velocities distribution and are compared with the previous work. The second part is about the BIW temperature and influence on the velocity field. Besides, the impact of the additional BIWs is assessed, regarding its impact on velocity and temperature fields. As for the oven behavior, the BIW results are also compared with the previous work.

CURE OVEN BEHAVIOR - Figure 7 shows the temperature profile of the cure oven at the end of the solution time for the current and previous work. The temperature profile is stable for the heating and cooling zones for both simulations. The heating zone shows a clear homogeneous temperature distribution with slight disturbances close to outlet ducts. The temperature distribution of the heating zone was close to 500 K throughout the whole simulation time. Only in the beginning when the BIW was cold, there were minor perturbations close to the BIW (see Section BIW behavior). The current result showed less temperature homogeneity close to the transition zone. That happened due to the increment of the inlet nozzles velocity, leading to temperature mixing between the cool and hot zones.

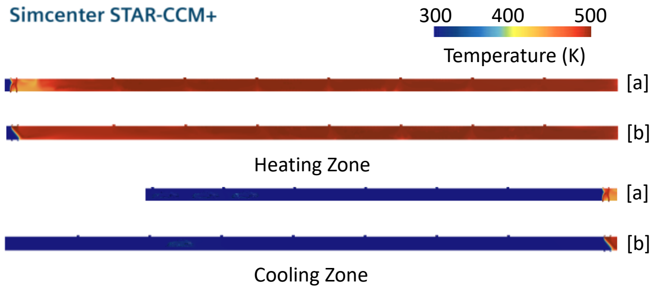

Figure 7. Cure oven temperature distributions of heating and cooling zones ([a] current work, [b] previous work).

The transition zone temperature distributions are presented in Figure 8. The previous result presented a clear threshold instead of a smooth transition between the heating and cooling zones. On the other hand, the current work presented a mixing effect. For both cases the designed transition zone nozzles were able to maintain an accepted isolation between the oven zones. The temperature average distribution close to the presented threshold is slightly lower than 500 K, since some mixing with the cooling zone is inevitable. Regarding the cooling zone, it showed a temperature distribution even more stable than the heating zone for both cases.

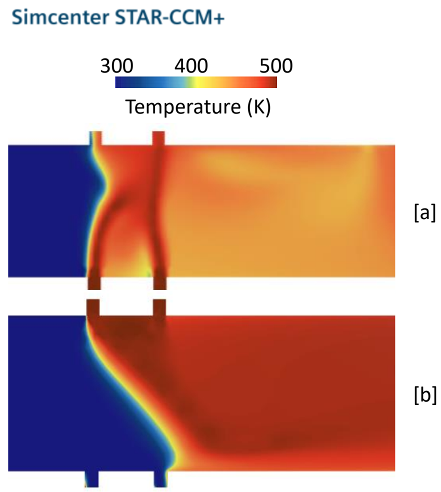

Figure 8. Cure oven temperature distributions of transition zone ([a] current work, [b] previous work).

The velocity flow distribution of the heating and cooling zones is shown in Figure 9. The heating zone does not show a noticeable pattern on the current result because of the transition zone changes. The previous result is affected by the transition zone flow pattern, but still with some homogeneity. The outlet ducts present higher velocities, enhancing turbulence effects near these regions for both simulations. The cooling zone showed a pattern around the outlet ducts for the previous study. This pattern is influenced by the transition zone high velocity flow. The current design presented more uniformity, but still with higher velocities close to the outlet ducts.

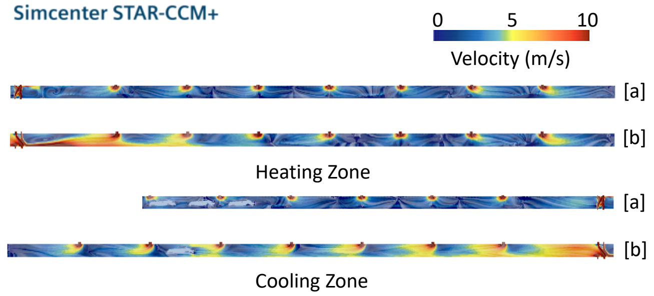

Figure 9. Cure oven velocity distributions of heating and cooling zones ([a] current work, [b] previous work).

The transition zone results are presented in Figure 10. This zone showed a large vortex towards the heating zone for both simulations, but the vortex is clearly smaller for the current work. Additionally, for the current design of the oven, the velocities around the vortex were lower, indicating more homogeneity, as shown in the temperature profile.

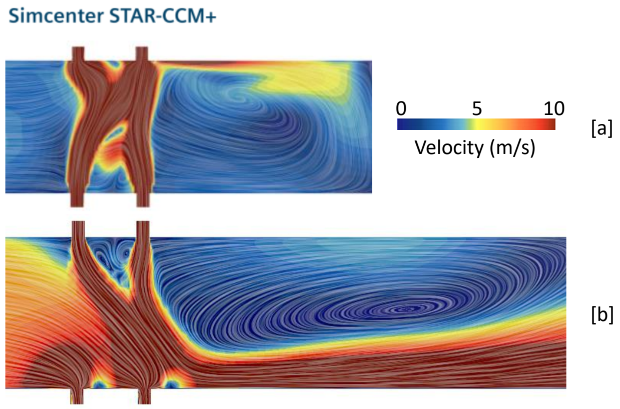

Figure 10. Cure oven velocity distributions of transition zone ([a] current work, [b] previous work).

BIW BEHAVIOR - The average temperature of selected parts of the BIW is presented in Figure 11. There is a clear difference between the results achieved by the optimized oven geometry and the previous one. The current geometry allowed the BIW to reach temperatures close to 20 K higher. Additionally, the current geometry showed faster heating and cooling. The time displacement between the results indicates the impact of the positioning of the additional BIWs. However, all the BIW parts showed the same behavior, a rise with a threshold close to 460 K for the previous geometry and 480 K for the current one. The heating part of the process presented an asymptotic pattern. On the other hand, the cooling part also showed an asymptotic pattern, however with inversed development.

The skid continued to absorb more heat than desired, particularly during the final phase of the heating process. Like previous findings, the skid and the roof reached higher temperatures and cooled more rapidly. The frame and the hood exhibited slower heating performance. This behavior is expected for the frame, as the parameter used is an average value, and the frame has the highest mass. Consequently, the frame had the highest temperature at the end of the simulated time due to its greater mass. The hood, however, did not experience recirculation around it, which reduced local heat transfer. The doors showed similar behavior, which was anticipated given the symmetry of the BIW and oven. This result is noteworthy as it allows for mesh simplifications in future assessments. The trunk exhibited behavior similar to the doors.

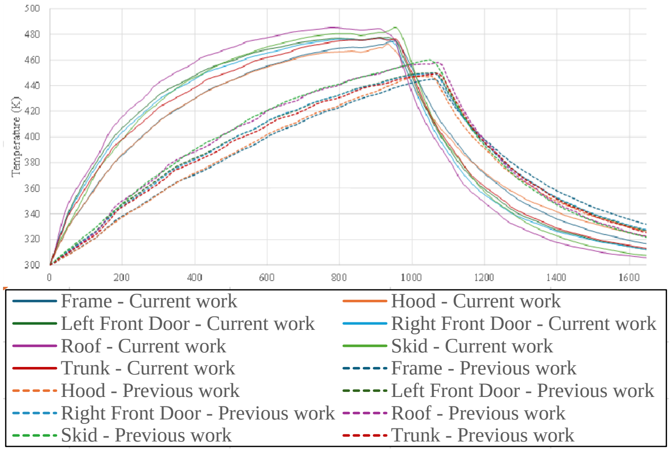

Figure 11. Average temperature evolution with time of selected BIW parts for current and previous works.

Figure 12 illustrates the flow around the BIW for both the current and previous geometries. The previous geometry reveals vortexes around the main components of the BIW, including the bottom of the frame, doors, and roof. However, there are two significant vortexes encompassing the skid, which are responsible for the high heat transfer to this part. The optimized geometry exhibits more vortexes around the components, facilitating higher heat transfer across the entire BIW (refer to Figure 8). Nonetheless, the current geometry still displays vortexes at the bottom of the frame, which enhance heat absorption by the skid. For future work, the diagonal nozzles will be removed from the oven, as they do not appear to provide any particular benefit.

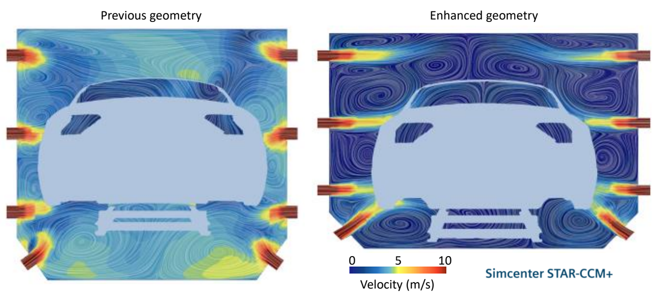

Figure 12. Flow around the BIW for the previous and current geometry.

Figure 13 shows the impact of the added BIWs on the flow around the monitored BIW (the one in the middle). In terms of the vortexes generated by the nozzles (see Figure 9), the added BIWs have a low impact. This is due to the distance between the BIWs, and this parameter impact will be addressed in future work. In terms of the axial flow, the BIWs accelerate the flow towards the next one. However, this acceleration comes with the downside of the heat transfer being enhanced in the first BIW to the second one and so on.

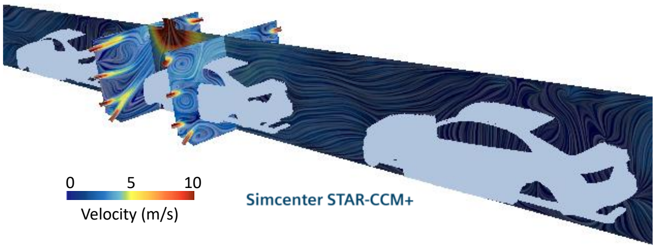

Figure 13. Additional BIWs impact on velocity distribution.

CONCLUSIONS

In the present research, a model of a paint oven was optimized and assessed utilizing Simcenter STAR-CCM+ [11]. This study aimed to minimize heat loss and enhance product quality. The initial model, which utilized a surrogate BIW with a refined overset mesh, identified significant heat transfer to the skid due to re-circulation near the transition zone. By redesigning the transition zone to change the flow direction from bottom to top, heat transfer to the BIW was enhanced, thereby reducing energy loss to the skid. Furthermore, adding more BIWs to the simulation helped to understand their mutual interactions, resulting in a more comprehensive and realistic depiction of the oven's performance under typical operational conditions.

The oven's behavior was primarily influenced by the air conditions provided by the inlet nozzles in all zones and the outlet ducts. This influence was also observed in the temperature distribution, which is noteworthy given the innovative redesign of the transition zone. The transition zone effectively isolated the heating and cooling zones, thereby improving energy efficiency by preventing air mixing.

The BIW performed as expected, heating to temperatures suitable for curing automotive paint and then cooling down, nearly returning to its initial temperatures. The heating and cooling phases exhibited asymptotic behavior with inverse trends, likely due to the differing flow patterns between the heating and cooling zones.

In summary, the use of Computational Fluid Dynamics (CFD) simulations in the automotive paint curing process leads to significant improvements in oven manufacturing, paint shop processes, and the quality of the final product. By leveraging CFD capabilities, automotive manufacturers can achieve enhanced productivity, superior oven performance, and ultimately deliver vehicles of exceptional quality to their customers.

REFERENCES

1. Cavalcante, Esley Silva, et al. "Automotive painting process: Minimizing energy consumption by using adjusted convective heat transfer coefficients." *Progress in Organic Coatings*. Vol 140. 2020.
2. Despotovic, Milan, and Milun Babic. "Analysis of different scenarios of car paint oven redesign to achieve desired indoor air temperature." *Energy Efficiency*. Vol 11. 2018.
3. Rao, Preetham, and Sreekanth Teeparthi. "A semi–computational method to predict body temperatures in an automotive paint bake oven." *ASME International Mechanical Engineering Congress and Exposition*. Vol. 54891. 2011.
4. Choi, Jongrak, Nahmkeon Hur, and Hee-Soo Kim. "A Numerical Simulation on the Fluid Flow and Heat Transfer Around a Vehicle in a Paint Drying Process." *Fluids Engineering Division Summer Meeting*. Vol. 55546. American Society of Mechanical Engineers, 2013.
5. Ashrafizadeh, A., R. Mehdipour, and M. Rezvani. "An efficient and accurate numerical simulation method for the paint curing process in auto industries." *Proc. International Conference on Applications and Design in Mechanical Engineering (ICADME), Penang, Malaysia*. 2009.
6. Pendar, Mohammad-Reza, et al. "Review of coating and curing processes: Evaluation in automotive industry." *Physics of Fluids*. Vol 34. 2022.
7. Choi, Jongrak, Giyeob Yang, and Nahmkeon Hur. "A numerical simulation of a line-type paint drying furnace." *International Journal of Numerical Methods for Heat & Fluid Flow* 30.5 (2019): 2639-2653.
8. Vieira, Tiago Augusto Santiago, et al. *CFD Analysis of the Paint Shop Curing Process.* SIMEA, 2024
9. Vieira, Tiago Augusto Santiago, et al. *A Computational Fluid Dynamics Methodology to Predict Automotive Painting Process Using Simcenter STAR-CCM+*. No. 2023-36-0056. SAE Technical Paper, 2024.
10. Rao, Preetham P., and Ashok Gopinath. "Energy savings in automotive paint ovens: a new concept of shroud on the carriers." *Journal of Manufacturing Science and Engineering* 135.4 (2013): 045001.
11. Siemens Digital Industries Software. Simcenter STAR-CCM+, version 2023.2, Siemens 2023.
12. Rao, Preetham P. "A heat exchanger analogy of automotive paint ovens." *Applied thermal engineering* 61.2 (2013): 381-392.